

# Calculation of Induction Motor Starting Parameters Using MATLAB

<sup>1</sup>Dejan Pejovski, <sup>2</sup>Bodan Velkovski

Undergraduate students

“Ss. Cyril and Methodius” University, Faculty of Electrical Engineering and Information Technologies  
Skopje, Republic of Macedonia

<sup>1</sup>dejan.pejovski@hotmail.com <sup>2</sup>velkovski\_bodan@live.com

**Abstract**—Squirrel cage induction motors are widely used in electric motor drives due to their satisfactory mechanical characteristics (torque, current, overloading) and small dimensions, as well as their low price. When starting an induction motor, a large current is required for magnetizing its core, which results in a low power factor, rotor power losses and a temperature rise in the windings. None of these parameters should reach values beyond certain limits until the motor reaches nominal speed, i.e. during the motor’s starting time. In this paper a comparison between two induction motors for a particular working mechanism will be presented. The choice will be based on three criteria: the motor’s starting time, winding temperature according to the insulation class, and rotor energy losses. The simulation is carried out with a specially developed tool in the MATLAB software environment.

**Key words**-induction motor; starting time; rotor losses; winding temperature; MATLAB

## I. INTRODUCTION

A large part of electrical energy is converted into mechanical energy in electric motor drives. Among different types of electric motors, induction motors are the most used for both home appliances and in various industries [1]. They are considered as workhorses in modern industry, because of their small size, low production and maintenance costs, wide power range, reliable operation etc. Three phase induction motors present (67 – 87) % of all installed AC drives [4]. This is so because they have been traditionally fed directly from the three phase AC electric power grid through electromagnetic power switches with adequate protection [1]. Typical motor applications include pumps, fans, compressors, mills, extruders, refiners, cranes, conveyors etc. [3]. This paper will present the design of a tool in MATLAB which is used to calculate the starting time, rotor energy losses and the winding temperature of a chosen electric motor for a given load represented by its torque-speed curve. In this paper, this tool will be used to compare the performance of two electric motors when used to propel a fan mechanism and to select the appropriate motor based on the results. The theoretical outline of the principle of operation of the designed tool will also be presented.

## II. METHODS OF STARTING AN INDUCTION MOTOR

Ideally, a motor-starting study should be done prior to purchase of a large motor. The manufacturer should provide the starting voltage and current values. A detailed study is necessary if the motor power exceeds 30% of the supply transformer(s) base kVA rating, if no generators are present. In some cases, if the motor power exceeds (10–15) % of the connected generator kVA rating, such analysis is also required [2].

Starting refers to speed, current, and torque variations in an induction motor when fed directly or indirectly from a rather constant voltage and frequency local power grid. A “stiff” local power grid means rather constant voltage even with large starting currents in the induction motors with direct full-voltage starting [1]. At zero speed at steady state, 6 to 8 times rated current is expected [8]. Full-starting torque is produced in this case and starting over notable loads is possible. For starting under heavy loads, a large design kVA power grid is necessary. On the other hand, for low load starting, less stiff local power grids are acceptable. Voltage decrease due to large starting currents will lead to a starting torque, which decreases with voltage squared, as shown in eq. (1) [1], [8].

$$M_p = \frac{3U_{1f}^2 R_2'}{\omega_0 s \left[ \left( R_1 + \frac{R_2'}{s} \right)^2 + (X_1 + X_2')^2 \right]} \quad (1)$$

$U_{1f}$  – voltage applied to each stator phase [V]

$R_1, R_2'$  – stator and rotor active resistances [ $\Omega$ ]

$X_1, X_2'$  – stator and rotor inductive resistances [ $\Omega$ ]

$\omega_0$  – synchronous angular speed [rad/s]

$s$  – slip, i.e. relative difference between motor’s synchronous speed and rotor speed.

To maintain the induction motor starting current at an acceptable range, the motor maximum power limit is calculated for a particular local power grid. The main negative effects that large starting current can cause are: notable stress in the electrical installations, great voltage drops, and the motor starting could be unsuccessful [8]. Various techniques have

been developed for starting large cage induction motors with allowable voltage drops and starting currents.

#### A. Direct starting

Direct induction motor starting is suitable and widely used for cage motors with small and medium power. This method is very simple, requires minimum additional equipment and is most economically acceptable. The starting current is 3 – 8 times above nominal, with low power factor and relatively small starting torque  $M_p$ . Neglecting the skin effect, eq. (2) describes the relationship between the motor current and the torque produced [8]. The rotor slip for rated motor speed is  $s_n=(0.5-8) \%$ .

$$\frac{M_p}{M_n} = \left( \frac{I_p}{I_n} \right)^2 \cdot s_n \quad (2)$$

Even in a rather stiff power grid, a voltage drop occurs during motor acceleration, due to the large current. A 10 % voltage reduction in such cases is usual [1]. In table 1 are presented common current and torque values when the induction motor is directly connected to the power grid [9]. These values refer to normal cage motor construction and rated power from 5 to 100 kW. An increase in starting current and a decrease in starting torque could be obtained with special motor constructions, such as double-cage or deep bar rotor [8].

TABLE I. TYPICAL CURRENT AND TORQUE VALUES FOR DIRECT STARTING OF AN INDUCTION MOTOR

n (rpm)	$I_p / I_n$	$M_p / M_n$	$M_{max} / M_n$
1500	6.5 – 6	1.4 – 1.1	1.8
1000	6	1.3 – 1.1	1.8
750	5.5	1.1	1.6

#### B. Wye-delta starting

The motor's stator winding is designed for delta operation and is star connected during the starting period. When the rated speed is reached, a changeover switch reconnects the stator winding from star to delta. With star connection, the stator phase voltage and phase current are reduced by  $\sqrt{3}$ , which means the torque and the line starting current are three times smaller compared to delta starting. This method is unsuitable for motors connected to loads that require a large starting torque [2], [9].

#### C. Stator resistance starting

In the stator resistance method, external resistances are connected in series with each phase of stator windings during starting. This causes voltage drop across the resistances so that the voltage available across motor terminals is reduced to (60–70) % of the nominal voltage [2], [9]. The starting resistances are gradually cut out in steps from the stator circuit as the motor speed rises until it reaches rated speed. The main disadvantages of this method are low starting torque and

increase in accelerating time, with power losses in the additional resistances [2].

#### D. Autotransformer starting

Instead of external resistances, an autotransformer can be used for connecting the motor to the power grid. The voltage is reduced to (55–75) % of its nominal value [2]. In induction motors, this causes current and torque decrease. The torque decreases proportionally to the voltage squared, which is acceptable only for large motors (MW range) and with light high starting loads, such as fans, ventilators, pumps etc. [1].

### III. STARTING TIME CALCULATION

At zero speed, when voltage is applied to the stator terminals, the stator current generates rotating magnetic field. This field induces electromotor force in the rotor squirrel-cage bars and a large rotor current starts flowing. As a result of the interaction between the rotor current, and the stator magnetic field, an electromagnetic force, i.e. torque is generated, which causes the rotor to start accelerating. The speed increases with the motor torque. Motor comes to rated speed which is near to its synchronous speed and the time taken to reach this point is called starting time [2], [10].

Equation (3) shows the torque equilibrium: at any point in dynamic state, the torque generated by the motor ( $M_m$ ) must equal the sum of load torque ( $M_s$ ) and the dynamic torque ( $M_d$ ) which accelerates or decelerates the rotor. Generic mechanical characteristics are shown in fig. 1 [11].

$$M_m = M_s + M_d = M_s + J \frac{d\omega}{dt} \quad (3)$$

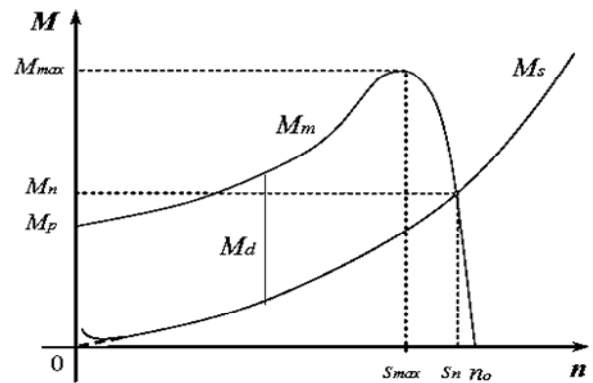


Figure 1. Motor and centrifugal load mechanical characteristics

If the relationship between angular and mechanical speed is taken into account, the dynamic torque can be computed as in eq. (4), where  $mD^2$  [kg·m<sup>2</sup>] is the motor centrifugal mass.

$$M_d = J \frac{d\omega}{dt} = \frac{mD^2}{38,2} \cdot \frac{dn}{dt} \quad (4)$$

Integrating eq. (3), the starting time can be calculated, as shown in eq. (5), where  $n_o$  [ $\text{min}^{-1}$ ] is the synchronous speed.

$$t_p = \int_0^{n_0} \frac{mD^2}{38,2(M_m - M_s)} dn. \quad (5)$$

Solving eq. (5) can be very complicated, especially when the motor starts with different load type, described with its mechanical torque  $M_s$ . A graphical approach has been developed for simplifying the integrating process [8]. Also a numerical method can be used, and the solution precision will depend on the number of steps taken into account. In this paper, the starting time calculation is based on Simpson's rule for parabolic interpolation, if the synchronous speed is equally divided into integer values in each step. Otherwise, a trapezoidal rule is used. The motor torque for each speed value is calculated by simplified Kloss equation (6), in which  $M_k = M_{max}$  [N] is the maximum (breakdown) torque, and the slip  $s_k = (5-25)$  % refers to the maximum torque point. The rotor slip  $s$  is computed according to eq. (7) [9].

$$M_m = \frac{2M_k}{\frac{s}{s_k} + \frac{s_k}{s}}. \quad (6)$$

$$s = \frac{n_0 - n}{n_0}. \quad (7)$$

The Kloss equation (6) can be accurately used for wound induction motors, and cage induction motors with negligible skin effect. Otherwise, it can be used only in the linear region of motor's mechanical characteristics, i.e. relatively small slips [8].

When the load torque is notable from zero speed on ( $>0.5M_m$ ) or the inertia is large ( $J_{vk} > 3J_m$ ), the starting process is slower and the machine may be considered to advance from steady state to steady state until full-load speed is reached in a few seconds to minutes (in large motors) [1].

#### IV. ENERGY LOSS DURING STARTING TIME

Starting an induction motor is actually a transient process similar to short circuit, because of the large stator and rotor currents. Due to these currents, much more electrical energy is used from the power grid during dynamic processes than in steady state. Depending on the load type, the energy losses in copper windings result in windings temperature rise and low drive efficiency. The rotor losses can be computed according to eq. (8), and the eq. (9) shows the total energy consumed by the induction motor during starting period [8], [9].

$$A_{Cu2} = \frac{mD^2}{365} \int_0^{n_0} \frac{M_m}{M_m - M_s} (n_0 - n) dn. \quad (8)$$

$$A_{rot} = \frac{mD^2}{365} n_0 \int_0^{n_0} \frac{M_m}{M_m - M_s} dn. \quad (9)$$

The kinetic energy generated in the motor rotating part is:

$$A_k = A_{rot} - A_{Cu2}. \quad (10)$$

According to eq. (8), (9) and (10) it can be calculated that the rotor winding losses during motor acceleration under no load are equal to the rotor kinetic energy at ideal no-load speed [1]. If the motor starts with mechanical load connected to its shaft ( $M_s \neq 0$ ), the rotor losses become even greater. This situation can be improved using variable speed drives. In fig. 2 energy balance is shown when the motor has one speed winding a), and when a Dahlander's winding is used for two different synchronous speeds in ratio 1:2 b). It is notable that in the second case the rotor losses are half the previous ones. In case c) a continuous speed change is shown, theoretically with no rotor losses [6].

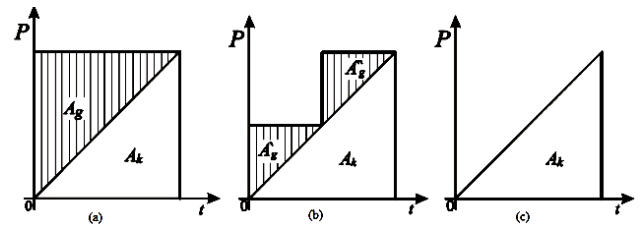


Figure 2. Power losses during induction motor starting: with one stator winding (a); Dahlander's winding speeds in ratio 1:2 (b); continuous speed change (c).

#### V. WINDING TEMPERATURE DURING STARTING TIME

The temperature gained in electric motor is one of the crucial parameters which determine motor's rated power. Motor energy losses transform into Joules heat: a part of them is transferred to the environment, while the other part increases motor's temperature. Stationary state is reached when all the generated heat is transferred to the environment, i.e. the temperature has a constant value [4]. This situation occurs typically after  $4T_z$ , where  $T_z$  [s] is motor's temperature constant (eq. 11). Although its basic value is seconds, the temperature time constant  $T_z$  is usually measured in minutes for smaller, or in hours for larger motors [5].

$$T_z = \frac{mc}{Sh}. \quad (11)$$

$m$  – motor mass, [kg]  
 $c$  – specific thermal capacity, [J / kg · K]  
 $S$  – motor surface which transfers heat, [m<sup>2</sup>]  
 $h$  – heat transfer factor, [J / K · m<sup>2</sup> · s]

The insulation materials are subjected to thermal stress and ageing, which is not regenerative. That means when determining rated motor power, for voltage  $U_n \pm 5\%$  and  $f=50\text{Hz}$ , the maximum stationary temperature must be taken into account (at maximum ambient temperature 40°C and at heights below 1000 m) [4]. The more efficient cooling system is used, the higher load can be connected to the motor. Basically, the motor can be of open or closed type. Open motors have their own inner ventilator on the shaft, and closed types use ribs and ventilators on the outside [4].

$$\theta = \theta_m \left( 1 - e^{-\frac{t}{T_z}} \right) + \theta_o e^{-\frac{t}{T_z}}. \quad (12)$$

Eq. (12) describes windings temperature change over time, where  $\theta$  [°C] is the current motor temperature above ambient temperature,  $\theta_o$  [°C] is the motor temperature in the beginning of the acceleration, and  $\theta_m$  [°C] is the maximum motor temperature, which is considered to be reached after  $4T_z$ . By definition,  $\theta_o = 0$  [°C] [8].

The cooling process can be described with eq. (13), where  $T_{zo} = T_z / \beta$  [s] is the temperature time constant during motor's cooling, which takes into account motor's construction type by the correction factor  $\beta$ .  $\theta_p$  [°C] is the temperature at the process beginning [8].

$$\theta = \theta_p e^{-\frac{t}{T_{zo}}}. \quad (13)$$

A MATLAB simulation that computes the motor's temperature according to eq. (12) and (13) was developed, with respect to the constant and variable rotor losses ( $P_{Fe}/P_{Cu}$ ), maximum temperature allowed depending on insulation class ( $\theta_d$  [°C]), and motor duty cycle. As most typical duty cycles according to IEC 60034-1 standard are considered: continuous maximum rating (constant load, S1), short-time duty S2 and intermittent duty S3. The recommended values for short-time duty are: 10, 30, 60 and 90 min, and the recommended values for the intermittent factor  $\varepsilon$  for S3 are: 15, 25, 40 and 60 % [5].  $\varepsilon$  defines the load duration ( $t_r$ ) relative to the cycle time ( $t_{cik}$ ):

$$\varepsilon = \frac{t_r}{t_{cik}} = \frac{t_r}{t_r + t_o}. \quad (14)$$

## VI. MATLAB SIMULATION

The MATLAB simulation was used to calculate the starting time, rotor energy losses and the winding temperature of two different induction electric motors: Končar 5AZ 100LB-8 and Sever ZK 100 Ld-8 when propelling an axial fan: Končar VAAZ A 800-A L260L720 M100B14P0,9. The results from the simulation are presented below. The technical specifications of the electric motors are given in table III. The technical specifications of the fan are given in table II.

Fig.3 depicts the torque-speed curves of the Končar 5AZ 100LB-8 motor and the fan, whereas fig.4 shows the torque speed of the Sever ZK 100 Ld-8 and the fan. The torque-speed curve of the fan was derived from its technical specification. Knowing that the torque-speed curve of an axial fan is centrifugal i.e. the torque is proportional with the speed squared, the torque can be represented with the following equation:

$$M_s = M_{sn} \cdot \left( \frac{n}{n_n} \right)^2. \quad (15)$$

$n_n$  [min<sup>-1</sup>] is the fan's nominal speed, and  $M_{sn}$  [Nm] is the fan's nominal torque which can be calculated as:

$$M_{sn} = 9.55 \cdot \frac{P_{in}}{n_n}. \quad (16)$$

$P_{in}$  [W] is the fan's input power, or the power required by the motor at the shaft. The fan's nominal speed and input power are taken from its technical specification.

TABLE II. TECHNICAL SPECIFICATIONS OF THE FAN [13]

Fan	Končar VAAZ A 800-A L260L720 M100B14P0,9
Air flow [m <sup>3</sup> /s]	5.7
Total pressure [Pa]	191
Speed [min <sup>-1</sup> ]	720
Input power [kW]	1.05
Static pressure [Pa]	114
$\eta_e$ [%]	61.9

TABLE III. TECHNICAL SPECIFICATIONS OF THE ANALYSED MOTORS [11],[12]

Motor	$P_n$ [kW]	$n_n$ [min <sup>-1</sup> ]	$n_0$ [min <sup>-1</sup> ]	$\eta$ [%]	$\cos\phi$	$U_n$ [V]	$I_n$ [A]	$I_p/I_n$	$M_n$ [Nm]	$M_p/M_n$	$M_k/M_n$	$J_m$ [kgm <sup>2</sup> ]	$m$ [kg]	Winding insulation class
Končar 5AZ 100LB-8	1.1	700	750	73	0.62	400	3.5	3.7	15	2.1	2.4	0.0104248	23	F
Sever ZK 100 Ld-8	1.1	680	750	73	0.72	380	3.2	3.5	15.5	2	2.2	0.0127	34.6	F

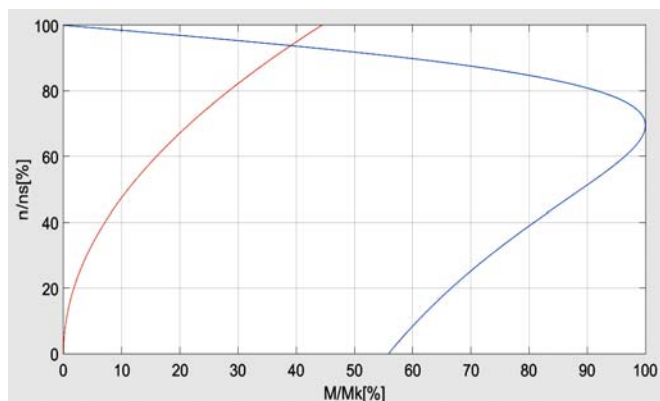


Figure 3. Torque-speed curves of the Končar 5AZ 100LB-8 motor and Končar VAAZ A 800-A L260L720 M100B14P0,9 fan.  $M_k=36.01$  [Nm];  $n_0=750$  [min<sup>-1</sup>]

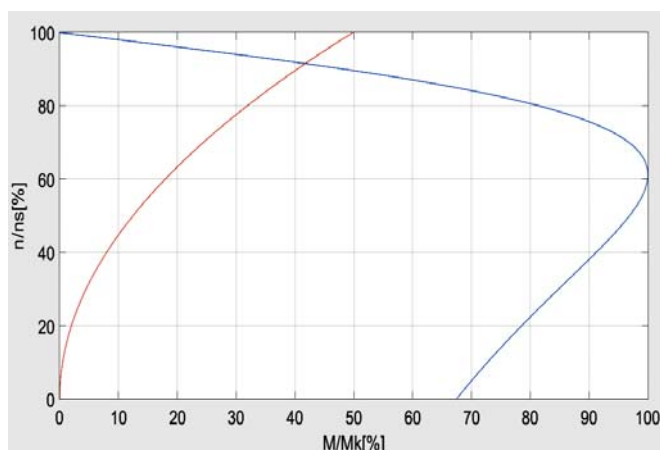


Figure 4. Torque-speed curves of the Sever ZK 100 Ld-8 motor and Končar VAAZ A 800-A L260L720 M100B14P0,9 fan.  $M_k=33.98$  [Nm];  $n_0=750$  [min<sup>-1</sup>]

#### A. Starting time calculation

Fig. 5 and fig. 6 illustrate the dependency between the starting time and the rotor speed of the Končar 5AZ 100LB-8 and Sever ZK 100 Ld-8 motors respectively. The starting time of the Končar motor is  $t_p=0.0387$ s and the starting time of the Sever motor is  $t_p=0.098$ s. The longer starting time of the Sever motor is due to its torque-speed curve which shows a greater starting torque. However, the torque starts to decrease at a lower speed, therefore this motor exhibits greater immediate acceleration, but then takes a longer time to reach the nominal speed.

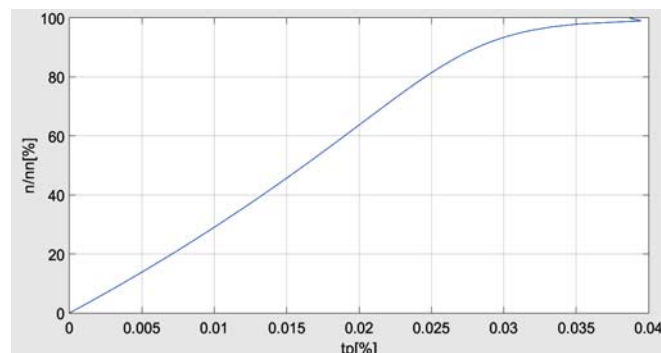


Figure 5. Speed-starting time curve of the Končar 5AZ 100LB-8 motor

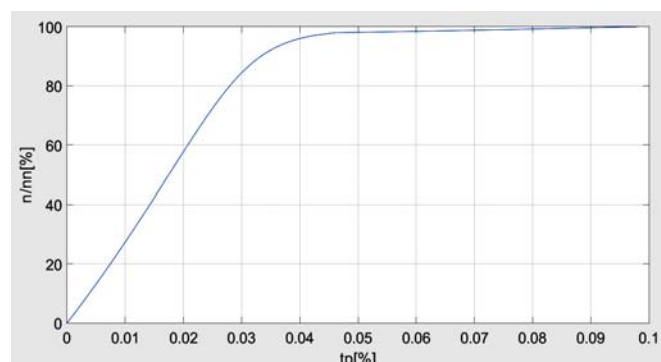


Figure 6. Speed-starting time curve of the Sever ZK 100 Ld-8 motor

#### B. Rotor energy losses calculation

The simulation also calculates the rotor energy losses –  $A_{cu2}$  [kWs], the kinetic energy generated in the rotor –  $A_k$  [kWs] and the total energy consumption –  $A_{rot}$  [kWs] of the two motors, which are presented in table IV. It is evident that the Končar motor is more efficient for the analyzed application. The kinetic energy generated in the rotor is smaller, due to its smaller mass, and more important, the energy losses in the rotor are smaller, which can also be deduced by the slope of the speed-starting time curve, shown in fig. 5.

TABLE IV. ROTOR LOSSES, KINETIC ENERGY GENERATED IN THE ROTOR AND TOTAL ENERGY CONSUMPTION OF THE MOTORS

Motor	$A_{cu2}$ [kJ]	$A_k$ [kJ]	$A_{rot}$ [kJ]
Končar 5AZ 100LB-8	34.207	15.7	49.915
Sever ZK 100 Ld-8	43.45	39.159	82.61

### C. Winding temperature calculation

As mentioned before, the simulation also calculates the windings temperature depending on the mechanism's duty cycle. This fan is intended to work in a continuous duty cycle – S1, as defined by IEC recommendations. This means that the motor works at a constant load, long enough to reach temperature equilibrium. Both motors are totally enclosed and fan cooled, and the insulation system in both is of an insulation class F, with a permissible temperature rise of 100 °C. The losses rate is  $P_{Fe} / P_{Cu} = 0.25$ , and the temperature time constant  $T_{\tau} = 10$  min.

Končar motor temperature rise is 92.89 °C, whereas the temperature rise of the Sever motor is 92.59 °C. Therefore, both motors satisfy their insulation class. The increase of winding temperature for each motor respectively is shown in fig. 7 and fig. 8.

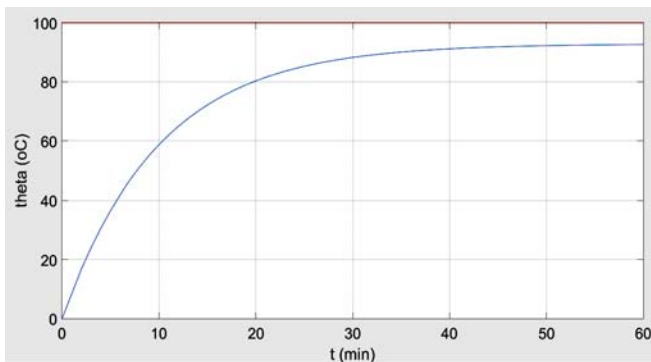


Figure 7. Temperature increase of the Končar 5AZ 100LB-8 motor

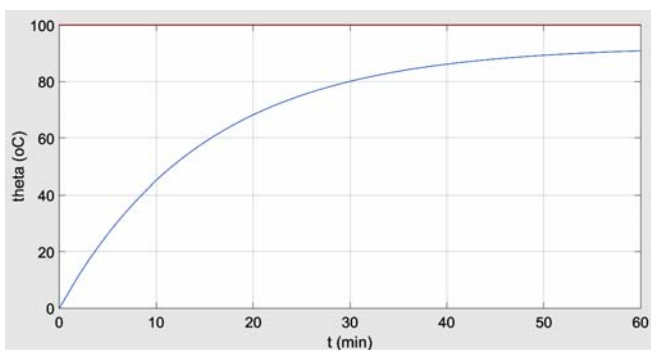


Figure 8. Temperature increase of the Sever ZK 100 Ld-8 motor

### VII. CONCLUSION

In this paper a MATLAB based tool was designed and presented, which calculates the starting time, rotor energy losses and winding temperature of an induction motor with respect to a given load. The tool's theoretical background was also presented. The paper's practical aim was to compare the performances of two machines when propelling an axial fan. The simulation results were presented and basing on its lower rotor losses as main criterion, faster starting time, and lower energy consumption, the Končar 5AZ 100LB-8 motor is proposed as the better machine for propelling the selected fan.

### GRATITUDE

The MATLAB tool presented in this paper was designed under the mentorship, guidance and extensive help of prof. dr. Slobodan Mirčevski and doc. dr. Mihail Digalovski for the purposes of the Laboratory of Electric Motor Drives, as a seminar work in the subject "Electric motor drives" at the Faculty of Electrical Engineering and Information Technologies in Skopje. The authors would like to express their immense gratitude to both of them.

### REFERENCES

- [1] Ion Boldea, Syed A. Nasar. "The induction machine handbook". CRC Press 2002
- [2] Abhishek Garg, Arun Singh Tomar. "Starting Time Calculation for Induction Motor". International Journal of Engineering Research and Applications, Vol. 5, Issue 5, (Part 3) May 2015, pp. 56-60
- [3] B. Venkataraman, et al. "Fundamentals of a Motor Thermal Model and its Applications in Motor Protection"
- [4] Zoran Stajih, hykan Vukih, Milam Radih. "Asinhronne masine". Elektronski fakultet u Nišu, 2012
- [5] K.C.Agrawal. "Electrical Power Engineering Reference & Application Handbook". CRC Press, 2007.
- [6] Slobodan Mirčevski. "Energy Efficiency in Electric Drives". 16th International Symposium on Power Electronics-Ee 2011, Novi Sad, Republic of Serbia
- [7] Berislav Jurković. "Elektromotorni pogoni". Školska knjiga, Zagreb, 1978
- [8] Branko Mitraković. "Asinhronne mašine". Naučna knjiga, Beograd, 1975
- [9] L. M. Piotrovski. "Električki strojevi". Tehnička knjiga, Zagreb, 1967
- [10] Prof. dr.sc. Ivan Gašparac, doc.dr.sc. Damir Žarko, prof. dr. sc. Drago Ban. "Elektromotorni pogoni s izmjeničnim motorima". predavanja, FER Zagreb, 2011/12
- [11] Končar. "Trofazni kavezni asinkroni motori".
- [12] Sever. "Low voltage three phase TEFC cage motors LV10EN".
- [13] Končar. "Ventilatori".